

Accepted manuscript

doi: 10.1680/jbibn.18.00005

Accepted manuscript

As a service to our authors and readers, we are putting peer-reviewed accepted manuscripts (AM) online, in the Ahead of Print section of each journal web page, shortly after acceptance.

Disclaimer

The AM is yet to be copyedited and formatted in journal house style but can still be read and referenced by quoting its unique reference number, the digital object identifier (DOI). Once the AM has been typeset, an ‘uncorrected proof’ PDF will replace the ‘accepted manuscript’ PDF. These formatted articles may still be corrected by the authors. During the Production process, errors may be discovered which could affect the content, and all legal disclaimers that apply to the journal relate to these versions also.

Version of record

The final edited article will be published in PDF and HTML and will contain all author corrections and is considered the version of record. Authors wishing to reference an article published Ahead of Print should quote its DOI. When an issue becomes available, queuing Ahead of Print articles will move to that issue’s Table of Contents. When the article is published in a journal issue, the full reference should be cited in addition to the DOI.

Accepted manuscript
doi: 10.1680/jbibn.18.00005

Submitted: 21 February 2018

Published online in 'accepted manuscript' format: 06 June 2018

Manuscript title: Generation of Nanomagnetic Biocomposites by Genetic Engineering of Bacterial Magnetosomes

Authors: Frank Mickoleit, Dirk Schüler

Affiliation: Dept. Microbiology, University of Bayreuth, Bayreuth, German.

Corresponding author: Dirk Schüler, Dept. Microbiology, University of Bayreuth, Universitätsstraße 30, 95447 Bayreuth, Germany. Tel.: +49(0)921-552729

E-mail: dirk.schueler@uni-bayreuth.de

Abstract

Magnetosomes are magnetic nanoparticles biomineralized by magnetotactic bacteria. They consist of a monocrystalline magnetite core enveloped by the magnetosome membrane, which harbours a set of specialized proteins. For the alphaproteobacterium *Magnetospirillum gryphiswaldense*, genetic techniques were developed to engineer both crystal morphology and the enveloping membrane, thereby generating building blocks for magnetic organic-inorganic hybrid materials. Genetic manipulation of magnetite biomineralization enabled the generation of core-engineered nanoparticles with adjusted magnetic and physico-chemical properties. Functionalization of the particle surface was achieved by genetic expression of enzymes and peptides genetically fused to abundant magnetosome anchor proteins. High-level expression allowed the generation of multifunctional nanoparticles with maximized protein-to-particle ratios. This allowed to tune surface properties (charge, hydrodynamic diameter), and the colloidal and enzymatic stability was improved by coating with inorganic and organic shells. The expression of molecular connectors might serve as scaffolds for the introduction of further functionalities. Overall, this demonstrates that the “synthetic biology” approach enables the generation of multifunctional, magnetic hybrid materials with a tuned property spectrum exceeding those of conventional materials, and the combination of different biogenic materials generates fully genetically encoded biocomposites with enhanced potential for various biotechnological and biomedical applications.

1. Introduction

Magnetosomes of magnetotactic bacteria (MTB) are a particularly intriguing example of genetically controlled *in vivo* synthesis of a magnetic biomaterial.¹ These membrane-enveloped nanoparticles (Figure 1) are evolutionary optimized for magnetic navigation by their well-defined size, shape, and composition, as well as their self-assembly into ordered nanochains.^{2,3} Magnetosome biosynthesis is compartmentalized within vesicles of the magnetosome membrane (MM) that provide confined “nano-reactors” in which the physico-chemical conditions are strictly regulated by a set of highly specialized proteins.⁴ These exert precise control onto different stages of biomineralization, resulting in exceptionally well-defined magnetic nanoparticles (MNP) with unprecedented properties (such as high crystallinity, strong magnetization, and uniform shapes and sizes).^{5,6} Biogenic magnetic nanoparticles were shown to exhibit properties superior compared to inorganic, chemically synthesized particles. For instance, magnetosomes from *Magnetospirillum gryphiswaldense* (Figure 1) were effectively tested as contrast agents for the two predominant magnetic imaging techniques MRI (*magnetic resonance imaging*) and MPI (*magnetic particle imaging*). In both applications, bacterial magnetosome particles outperformed all other tested magnetic particle formulations, and in particular were superior to *Resovist*, the current commercial “gold standard” material.⁷⁻⁹ In addition, fluorochrome-coupled bacterial magnetic nanoparticles have been used as fluorescent bimodal contrast agents for stem cell tracking,^{10,11} and when used for hyperthermia, magnetosomes exhibited higher absorption rates, more uniform heating (in

particular for magnetosome chains) and exceptionally large values for real magnetic losses.^{12,13} However, the application potential of bacterial magnetosomes would be further advanced by the introduction of additional functionalities. Intriguingly, both crystal morphologies and the composition of the enveloping magnetosome membrane can be manipulated at the genomic and proteomic level. These features make them ideal for many biomedical and biotechnological applications. In the following, we describe recent approaches for genetic engineering of biogenic MNP in the magnetotactic alphaproteobacterium *M. gryphiswaldense*. Versatile expression cassettes enabled high-yield magnetosome expression of foreign proteins and peptides. Overall, prerequisites were thereby generated not only for the bioproduction of core-engineered MNP with tailored magnetic and physico-chemical properties, but also for the generation of building blocks for multifunctional organic-inorganic hybrid materials by synthetic biology.

2. Overview of genes functional in magnetosome biomineralisation

Engineering of magnetosomes takes advantages of the fact that all steps of biosynthesis are under genetic control of >30 specific genes. In *M. gryphiswaldense*, these are clustered mostly within a large conserved genomic magnetosome island (MAI) comprising the *mms6*, *mamGFDC*, *mamAB*, *mamXY* and *feoAB1* operons (Figure 2A).^{3,14,15} The *mamAB* operon is the only region of the MAI, which is necessary and sufficient for magnetite biomineralization.¹⁵ Studies of deletion mutants revealed several essential and nonessential genes involved in various steps of magnetosome biosynthesis: Only *mamE*, *-L*, *-M*, *-O*, *-Q*, and *-B* were essential

for formation of magnetite, whereas a *mamI* mutant still biomineralized tiny particles which, however, consisted of the nonmagnetic iron oxide hematite. A model for magnetosome biosynthesis in *M. gryphiswaldense* is shown in Figure 2B.^{3,16} Magnetosome biosynthesis depends on different steps including various magnetosome proteins. The key proteins MamB, MamM, MamQ and MamL mark the beginning of a recruitment cascade and are required to position a network of additional magnetosome proteins, including MamI, MamE and MamO. In turn, recruitment of further magnetosome proteins (and oligomerization into high molecular weight complexes) may introduce curvature into the cytoplasmic membrane. MamB was found most important for MM formation, and it might act as the initial landmark protein to prime complex formation at certain sites within the cytoplasmic membrane. After a critical size and composition of the multi-protein assembly is reached, the formed lipid-protein complex induces rapid invagination to form the magnetosome lumen.¹⁷ After vesicle formation (by detachment of the MM), ferrous iron is transported into the magnetosome vesicles by MamB and MamM.¹⁸ Ferric iron is taken up by MamH and MamZ¹⁹ or formed by oxidation of ferrous iron within the vesicles. MamI is involved in magnetite nucleation. MamO was speculated to be directly involved in precipitation of iron oxide particles. The crystal growth is affected by several magnetosome proteins, including MamE, which was shown to proteolytically remove growth inhibitors or activate growth-promoting proteins in the related *M. magneticum*.²⁰ Based on the conserved CXXCH heme-binding motifs within MamE, MamT, MamP, and MamX, it has been speculated that the proteins form a complex for electron transport to regulate electron flow.^{19,21} MamS and MamR control crystal size by a yet unknown mechanism. MamN exhibits

similarity to H⁺ translocation proteins and might be involved in crystal growth by regulating intra-magnetosomal pH.¹⁴ Mms6 is specific to magnetotactic bacteria. It is tightly bound to the magnetosome crystals²² and thought to form stabilizing interactions with magnetite surfaces during crystal growth.²³ Mms48 and Mms36 act as inhibitors of crystal growth or recruit inhibiting proteins of particle growth by an unknown mechanism. The small, hydrophobic proteins MamG, MamF, MamD, and MamC control in a cumulative manner the growth of magnetite crystals.²⁴

Magnetosomes are subsequent aligned into ordered chains through the interaction of MamJ on the magnetosome membrane with a cytoskeletal filament that is formed through the polymerization of the actin-like MamK. The latter is furthermore required for the positioning of the particle chain at midcell.^{25,26} Organization of magnetosomes into chains helps to align individual magnetic dipoles to generate a strong dipole that can ‘sense’ the geomagnetic field.³

3. Genetic engineering of magnetite cores with tuned magnetic properties

Magnetic properties of magnetosomes are critically dependent on their size: While particles smaller than about 30 nm were superparamagnetic (SP, no permanent magnetic signal at room temperature in the absence of an external field) and were less prone to magnetic agglomeration, particles between 30 and 60-100 nm are stable single domain (SSD, one domain, remanent magnetization) (Figure 3). (Engineered) large single domain particles (LSD) represent an optimum, close to maximal coercivity, and particles larger than 100 nm being multidomain (MD, more than one domain, have remanent but reduced volume magnetization compared to SSD).^{27,28}

Thus, as magnetic properties of magnetosomes critically vary over a rather narrow size range, either superparamagnetic or ferrimagnetic (including large single domains) particles could be deliberately selected by size control.

Deletion of several single *mam* genes or entire operons resulted in strains that were affected in magnetosome biosynthesis. Since the *mamGFDC*, *mms6* and *mamXY* operons have crucial (and partially overlapping) functions for the formation of functional magnetosomes, deletions of the corresponding operons affected the morphology, size and organization of magnetite crystals, and some of the mutant particles displayed modified shapes, such as elongated and needle-like crystallites.¹⁵

A set of genetically engineered *M. gryphiswaldense* strains producing magnetosome crystals between 15 and 46 nm (mean size) and size increments between 2-5 nm was generated (for examples see Figure 3). Most modifications caused the formation of smaller magnetite crystals. Purified magnetosomes were, for instance, analyzed by FORC (first order reversal curves) which confirmed that smaller particles (as exemplified by strain Δ F3D, average crystal size = 23.6 nm; Figure 3) display true superparamagnetic (SP) behavior, whereas characteristics of unmodified WT particles were compatible with a mixture of SSD and SP particle sizes. However, deletion of the *mms48* and *mms36* genes resulted in fewer, but significantly larger crystals, falling into the large single domain (LSD) size range, which is expected to be associated with exceptional, but so far mostly unexplored magnetic properties. Thus, particles isolated from strain Δ *mms48* (diameter = 41 nm) showed higher coercivity, displayed the strongest and irreversible magnetization and stable single domain behavior.^{7,27} In

addition, modular overexpression of multiple magnetosome genes resulted in the generation of larger-than-WT particles, with a gradual size increase of crystals up to 80 nm.²⁹ Extra copies of magnetosome genes or gene clusters were transferred to *M. gryphiswaldense* and chromosomally inserted by transposition. Introduction of an additional copy of the *mms6* operon into strain IK-1 ($\Delta recA$, to prevent recombination between identical copies)³⁰ resulted in particles whose mean size was increased from 35 nm to >45 nm. These results are promising for the future bioproduction of size-adjusted larger monocrystalline magnetic nanoparticles (LSD). Thus, magnetic characteristics (i.e. magnetization, coercivity, domain state) can be engineered by genetic control of particle size.

4. Multi-functionalization of bacterial magnetosomes by synthetic biology approaches

4.1 Codon optimization and versatile expression cassettes allow high-level display of foreign peptides

Chemical surface functionalization of non-biologically produced magnetic nanoparticles was shown to improve their colloidal stability, allowed the generation of bioconjugates, and enabled selective recognition and binding of targets.³¹ For magnetosomes, *in vivo* functionalization by genetic engineering provides a number of advantages over chemical coupling, such as the full use of subtle biological control mechanisms, and the fact that the final product can be obtained within a single step by biosynthesis without any coupling chemistry. For the selective and stable magnetosome display of functional moieties in *M. gryphiswaldense*, translational fusions of the peptides of interest with highly abundant

magnetosome membrane proteins were generated. A well-established magnetosome membrane anchor is the 12.4-kDa MamC protein, which has only a minor function in magnetite biomineralization.^{24,32} Both its N- and C-terminus provide sites for covalent and highly specific attachment of foreign proteins to the magnetosome surface by genetic fusion.³³⁻³⁵ As an essential prerequisite, a genetic cassette was constructed which allowed the convenient cloning and magnetosome expression of any DNA-encoded peptide. Different developed promoter systems allowed either moderate induced or high constitutive expression. By using eGFP as a reporter, the native P_{mamDC} was identified as the strongest promoter functional in *M. gryphiswaldense*. Further optimization of P_{mamDC} by gradual truncation resulted in a minimal functional cassette of 45 bp (P_{mamDC45}), which displayed a threefold higher expression than the native P_{mamDC} . In addition, an optimal spacing between ribosomal binding site (RBS) and the start codon of 8 bp was revealed, which yielded a 2.8-4 fold higher fluorescence than other spacers.³⁴ Furthermore, introduction of a P_{Tet} promoter modified after *Bertram and Hillen (2008)*³⁶ was tested. P_{Tet} not only provided tight repression if uninduced, but also allowed a tunable, high expression upon induction. Expression levels were about 60% of that of P_{mamDC} after 6 h induction, but could be further increased by a prolonged induction.³⁴

Due to preferences in codon usage and the divergent %G+C content of *M. gryphiswaldense* genes (61.2%) compared to different eukaryotic systems (ca. 30-70%), magnetosome expression of foreign genes could be further enhanced by codon-optimization. For example, using the *egfp* gene as a model, expression and fluorescence of a codon-optimized variant (= *megfp*) was significantly improved (>30%).³⁴ In addition to

versatile expression cassettes, codon optimization might be therefore an important tool for high-level expression of foreign peptides.

4.2 Identification of highly abundant magnetosome proteins as membrane anchors

Magnetosome expression of higher amounts of foreign proteins had been limited by the maximum possible copy number of the magnetosome anchor MamC in the MM. Therefore, in order to identify further suitable membrane anchors, the exact composition and stoichiometry of the associated membrane integral proteins was analyzed by semi-quantitative mass spectrometry.³⁷ Acquired proteomic data was combined with previously published quantitative Western blot data,³² and the protein copy number and density within the magnetosome membrane could be modeled. This revealed that magnetosome proteins were present in different copy numbers (e.g., MamG: ~6; MamF: ~21; MamC: ~100) with up to 120 copies per particle (Mms6), which suggests an unusually crowded protein composition of the membrane.³⁷ Using both GusA (β -glucuronidase from *Escherichia coli*) and eGFP as reporters, the abundant MamF (tightly bound to the magnetosome membrane due to three TMHs), MamG and MamA (an abundant MM-associated proteins lacking TMHs, but bound to MM by electrostatic interactions)^{16,35} were explored to function as reliable membrane anchors. Generated fusions were analyzed with respect to exposure, expression and stability under various conditions by estimating reporter activity.³⁸

4.3 Genetic magnetosome expression of peptides, enzymes and functional groups

For many biomedical and biotechnological applications, the addition of functional moieties to

the particle surface is required. However, it remained unexplored until recently how the activity and stability of peptides or enzymes is affected by their magnetosome expression. In addition, potential applications (e.g. as magnetic sensors or as bi-/multimodal contrast agents) and functionalization of magnetosomes rely on densely decorated, catalytically active particles with maximized protein-to-particle ratios. For their subsequent use as building blocks for magnetic organic-inorganic hybrid materials, available techniques were combined to create a versatile and diverse genetic toolkit for the generation of “smart” multifunctional magnetic nanoparticles with plenty of tailored properties within *M. gryphiswaldense*. The feasibility of this approach was demonstrated by producing a set of different model particles (illustrated in Figure 4).

4.3.1 Expression of fluorophores and enzyme proteins

In order to explore the display of functional moieties or even multisubunit complexes, the magnetosome display of a chimeric bacterial RNase P enzyme was examined, a highly conserved ribonucleoprotein complex composed of the protein subunit (C5) of *Escherichia coli* RNase P and a single endogenous RNA subunit.⁴¹ C5 was fused to the C-terminal end of MamC via 13 residues of a flexible Gly-Ser linker to avoid steric hindrance, which could inhibit complex formation, and the fusion protein was efficiently expressed in *M. gryphiswaldense* under the control of P_{mamDC} promoter. Isolated C5 particles showed apparent RNase P activity (confirmed by analysis of the cleavage of pre-tRNA under physiological conditions). The endogenous RNase P RNA subunit could associate with the C5

particles, and reaction rates were comparable to those reported for the *E. coli* RNase P holoenzyme.⁴³ Thus, similar anchoring strategies might also be used for the generation of artificial multienzyme-like complexes for novel, completely artificial reaction pathways with high efficiency and accuracy.

Borg et al. (2014) showed that the genetic duplication of the eGFP protein fused in tandem to MamC resulted in enhanced and stable magnetosome fluorescence and an overall increased expression of the eGFP protein (up to 520 copies per particle).³⁴ The potential of this strategy was further investigated by magnetosome expression of multiple copies of the model enzyme GusA,³⁹ which in *M. gryphiswaldense* was previously used as transcriptional reporter to study promoter activities and gene regulation.^{34,44,45} Arrays of up to five GusA monomers plus an additional mEGFP were genetically stitched together and fused as a large hybrid protein to a single MamC anchor protein. Purified magnetosome particles exhibited mEGFP fluorescence and a stable, up to 2.8-fold increased specific activity compared to monomeric GusA protein expressed as single-copy magnetosome fusions. Furthermore, catalytic activities were almost linear, sequentially increased with the number of GusA monomers per array. In total, about 190 GusA monomers were covalently attached to individual particles. Assuming layers of GusA rows surrounding the particles, the monomers would thus cover up to 90% of the magnetosome surface.³⁹ This demonstrates that genetic multiplication is a very powerful strategy for high-level magnetosome expression of foreign polypeptides with maximized protein-to-particle ratios.

Furthermore, the integral, highly abundant MamF and MamG proteins as well as the

surface-bound MamA were investigated as further candidates to act as suitable membrane anchors that might enable the simultaneous display of multiple peptides. The subcellular localization of MamF and MamG (in addition to MamC) had been studied before by expression of eGFP-tagged versions of the corresponding magnetosome proteins.³³ Oxygen-limited growth conditions were established that ensured growth, magnetite biomineralization, and eGFP fluorophore formation at reasonable rates. Isolated magnetosomes expressing MamC-eGFP, MamF-eGFP, or MamG-eGFP displayed strong fluorescence, which was visualized by fluorescence microscopy in the form of bundles of chains. MamC-eGFP particles displayed the highest fluorescence, while the fluorescences of MamF-eGFP and MamG-eGFP magnetosomes were approximately threefold (MamF-eGFP) and fivefold (MamG-eGFP) lower. These data demonstrate not only the use of eGFP as reporter for expression and localization, but also the utility of MamF and MamG as anchors for magnetosome display of heterologous gene fusions.³³

For construction and magnetosome expression of bifunctional *mamC/A/F/G-gusA-megfp* fusions in the wild type or their respective deletion backgrounds ($\Delta mamC$, $\Delta mamA$, $\Delta mamF$ or $\Delta mamG$, respectively),³⁸ the optimized $P_{mamDC45}/oRBS$ expression systems was used as for MamC. mEGFP fluorescence intensities as well as GusA protein amounts and reaction rates correlated with the known abundance of the utilized membrane anchors (i.e. MamC > MamA > MamF > MamG^{32,37}). When studying GusA enzyme kinetics, low K_M constants were obtained, suggesting a high substrate affinity comparable to the cytoplasmic expressed enzyme. Similar values were also obtained for *mamC-gusA* fusions, which indicates that the additional mEGFP

copy does not influence catalytic activities. For the deletion strains $\Delta mamC/A/F/G$ lacking the respective wild type alleles mEGFP fluorescence intensities and GusA activities were nearly twice as high as for the corresponding wild type strains as expected. Since the latter harbour two copies of the corresponding *mam* gene (one unfused wild type copy and one additional *mam-gusA-megfp* fusion) it is likely that within the magnetosome membrane both versions are statistically distributed at a 50:50 ratio.³⁸

4.3.2 Magnetosome display of molecular connectors and antibodies

In addition to fluorophore- and enzyme-displaying particles, magnetosomes were engineered that express versatile coupling groups on the surface.^{40,46,47} The latter included small (~15 kDa) camelid antibody fragments (nanobodies), which unlike conventional antibodies bind their antigens via only a single variable domain fragment and fold rigidly. Magnetosome-specific expression of a red fluorescent protein (RFP)-binding nanobody (RBP) *in vivo* was accomplished by genetic fusion of RBP to the magnetosome protein MamC. Isolated magnetosomes expressing MamC-RBP efficiently recognized and bound their antigen *in vitro* and could be used for immunoprecipitation of RFP-tagged proteins and their interaction partners from cell extracts. Furthermore, co-expression of monomeric RFP and MamC-RBP resulted in intracellular recognition and magnetosome recruitment of RFP within living bacteria.⁴⁶ Moreover, RBP magnetosomes could be used for the generation of fluorescent assemblies of nanoparticles of varying types.⁴⁸ A fusion protein of MamK, which is known to form filaments *in vivo* and *in vitro*, and mCherry (a variant of the red fluorescent protein) was

recombinantly expressed and isolated using a hexahistidine tag that was subsequently used to bind functionalized gold nanoparticles to polymerized MamK_mCherry_His₆ filaments. The concomitant addition of RBP magnetosomes (capable of binding mCherry) resulted in fluorescent structures, which could be actuated by an external magnetic field. In addition, *Borg et al. (2015)* succeeded in expressing the gene for a GFP-binding nanobody (GBP, green binding protein, Chromotek Inc.).⁴⁷ GBP-expressing magnetosomes were further functionalized by a mCherry-GBP tandem fusion to facilitate visualization of mCherry-GBP magnetosomes by their red fluorescence. Moreover, the expression of multivalent GFP-binding nanobodies on magnetosomes has been used as an “intracellular nanotrap”, and the chemotaxis protein CheW₁-GFP could be retargeted from polar chemoreceptor clusters to the midcell, resulting in a gradual knockdown of aerotaxis. Conversely, entire magnetosome chains could be redirected from the midcell and tethered to one of the cell poles.

The biotin/streptavidin (SAV) system described for instance by *Ceyhan et al. (2006)*⁴⁹ and *Lang et al. (2007)*⁵⁰ turned out to be an intriguing alternative for specific coupling reactions. SAV-modified magnetosomes had already been used for the automated discrimination of single nucleotide polymorphism. The streptavidin-modified particles were coupled to biotinylated oligonucleotides to facilitate magnetic separation of DNA hybrids and used for the detection of single nucleotide polymorphisms.⁵¹

As the display of versatile coupling groups as hybrid proteins fused to MamC not only allows a controlled decoration of the magnetosome surface, but also enables specific binding to other nanoparticles presenting the corresponding complementary antigens or ligands,

functionalized magnetosomes (displaying GBP nanobodies or SAV monomers) were used to generate a new kind of biocomposite by specific coupling reaction with tobacco mosaic virus (TMV) particles.⁴⁰ Plant viruses like TMV have proven to be well-suited scaffolds and building blocks for the integration into hybrid materials^{52,53} as they exhibit a reproducible and narrow size distribution, high stability, defined shape and easy modifiability of the capsid proteins, which allows the coupling of a variety of molecules.⁵⁴ Furthermore, pre-synthesized magnetic nanoparticles have been shown to align along the axes of plant viruses,⁵⁵ and the amplified cumulative dipole can improve magnetic resonance imaging (MRI).⁵⁶ TMV particles were functionalized *in vitro* either with EmGFP (a variant of the green fluorescent protein) or biotin residues and allowed directed interactions with GBP or SAV magnetosomes.⁴⁰ Quantity and position of EmGFP or biotin turned out to be crucial for TMV-magnetosome complex formation. Thus, densely ‘decorated’ TMV allowed the formation of extensive mesoscopic, strand-like structures with the virus particles forming a scaffold for magnetosome binding. Depending on the particle amounts, strands of different size were formed, ranging from single-layered two- or three-chained to extensive multilayered microrods. These findings therefore demonstrated the flexibility of the approach as strand dimensions can be (roughly) directed and controlled by applying different TMV:magnetosome ratios. Furthermore, magnetosomes and TMV particles could effectively coupled at a distinct stoichiometry. Thus, coupling of 5’-plane functionalized TMVs (either presenting EmGFP or biotin residues at the ‘end’ of the TMV rod) with magnetosomes that display the corresponding complementary group (GBP or SAV, respectively) resulted in a high portion of 1:1 coupled TMV-magnetosome

‘drumsticks’, i.e. TMV rods were bound to one single magnetosome at the end of the rod.⁴⁰

This high control in coupling two different kinds of nanoparticles can only be achieved by genetic functionalization approaches as chemical strategies often lack high selectivity.

5. *In vivo* and *in vitro* coating strategies

5.1 *Expression of artificial spider silk-inspired peptides on the magnetosome surface*

The usability of bacterial magnetosomes in many applications could potentially be further improved by encapsulation in biocompatible organic polymers. An intriguing material suitable for organic/proteinaceous coatings could be spider silk, which exhibits extraordinary properties such as a high toughness combined with good biocompatibility⁵⁷⁻⁵⁹ desirable for future *in vivo* applications. *Mickoleit et al. (2018)* for the first time demonstrated that recombinant spider silk peptides can be expressed in *M. gryphiswaldense*.⁴² By designing engineered spider silk sequences (based on the conserved motif C of *Araneus diadematus* fibroin 4)^{60,61} for magnetosome expression, two strategies were explored: (i) Because it is known that glycine linkers may improve folding of recombinant fusion proteins and also reduce sterical hindrance,⁶² single C motifs were connected by Gly₁₀ and the resulting arrays with two or 32 silk units (referred to as CL2 or CL32, respectively) were genetically fused to MamC as membrane anchor (Figure 5). In addition, (ii) a linker-less construct with the established C2 peptide⁶³ stitched to MamC was generated, resulting in a MamC-C2 hybrid protein. The need of a seamless cloning strategy⁶⁰ preserving the highly repetitive hydrophobic character of silk proteins^{64,65} was experimentally confirmed as the introduced Gly₁₀ in constructs MamC-CL2

and MamC-CL32 affected the proteins properties and lead to affection of cell division, magnetosome production and protein expression. In contrast, magnetosome display of the linker-less C2 silk motif caused the formation of a proteinaceous coat with exposed spider silk features (specific interaction with eADF4(C16) spider silk protein) and thus provides a promising route for encapsulation of bacterial nanoparticles (Figure 5). Since spider silk is non-immunogenic,⁶⁶ in future applications such building blocks might improve the biocompatibility of bacterial magnetosomes and mask immunogenic compounds displayed on the particle surface. Furthermore, it could be demonstrated that the surface properties of magnetic nanoparticles can be tuned, as particle agglomeration was reduced (most likely because of negatively charged amino acid residues, e.g. glutamate residues of the silk motifs) and the colloidal stability significantly increased.⁴² Moreover, magnetosome expression of spider silk-inspired peptides could be used in future approaches to generate multifunctional nanoparticles that combine spider silk features with further functionalities, such as catalytic activities, and to produce magnetic silk composites that can be oriented and manipulated by an external magnetic field.⁶⁷

5.2 Fabrication of multicoated magnetic nanoparticles by peptide-directed and chemical synthesis of inorganic coatings

For the versatile generation of magnetic, multifunctional (hybrid) materials it was investigated whether particle-displayed, physico-chemical characteristics can be further improved by inorganic coating strategies. For chemical synthesis of silica encapsulated magnetosomes,

tetraethyl orthosilicate (TEOS) was precipitated in alkaline solution using isolated WT magnetosomes as precursor.⁶⁸ Incubation for 18-24 h resulted in the formation of single silica-shelled magnetosomes with a thickness of the capsule of about 60 nm (Figure 6). In the presence of static magnetic fields, up to twenty magnetosomes were often found to be collectively encapsulated by silica, forming chain-like magnetic structures, behaving as nano-bar magnets. If encapsulation was performed within the rotating field of a magnetic stirrer, individual separated Si-magnetosomes predominated over chained Si-magnetosomes. By variation of conditions during encapsulation (seed magnetosome concentration, absence/presence of ambient magnetic fields), the thickness of silica shells could be varied between 3 and 20 nm, and suspensions of either single silica-coated MNP or coated nanorods could be generated (Figure 6C). Fluorescence of eGFP-expressing magnetosomes was not only preserved during encapsulation, but coating significantly increased resistance of eGFP-magnetosomes against denaturation (1% SDS) and protease treatment and also prolonged shelf-storage. Encapsulated magnetosomes furthermore displayed higher colloidal stability than non-encapsulated particles, potentially caused by electrostatic repulsion (due to high negative zeta potential of encapsulated particles) and increased spacing, thereby reducing short-range interparticle magnetic interactions.⁶⁸ Because of their enhanced stability and expected decreased immunogenicity, the silica-coated eGFP-magnetosomes are promising as future bimodal magneto-fluorescent contrast agent for magnetic imaging of various biological processes, such as tracers for stem cells and tumors.¹⁰

As another strategy, *Borg et al. (2015)* investigated whether magnetosomes can be coated with zinc oxide.⁶⁸ For that purpose, magnetosomes expressing the ZnO-binding peptide 31 were genetically constructed. The latter was shown to exhibit a strong binding to ZnO with dissociation constants in the nanomolar range.⁶⁹ The peptide was expressed as a mixed MamC-eGFP-31 fusion, resulting in eGFP-31-functionalized magnetosomes.⁶⁸ ZnO coating (thickness ~20 nm) provided additional functions to the magnetic nanoparticles, since ZnO exhibits piezoelectricity⁷⁰ and is a semiconducting material with antimicrobial activity.⁷¹

6. Increasing magnetosome yields by optimization of growth conditions, generation of overproducer strains and magnetosome production in foreign hosts

In the past, the use of magnetosomes in real-world applications was limited by fastidious, slow growth of magnetotactic bacteria and poor particle yields. However, recent progress in improving cultivation has led to considerably increased magnetosome amounts and will enable mass production of functionalized magnetosomes. For instance, *Zhang et al. (2011)* reported high-density cultivation of *M. gryphiswaldense* in a large-scale fermentor.⁷² In addition to fermentation procedures based on oxygen respiration,⁷³ an alternative fermentation regime was developed, in which oxygen was gradually depleted to reach suboxic conditions favouring nitrate respiration. Magnetite biomineralization was substantially increased during denitrifying growth,⁴⁴ and although cell densities were lower compared to oxic growth (due to growth-limiting low concentrations of nitrate required to reduce its toxicity), the amount of synthesized magnetite was substantially increased by >50%.

Another tempting way to increase magnetosome yields and simplify bioproduction has been the use of genetic engineering to generate overproducing strains, or even transplantation of the entire magnetosome pathway to a more facile biotechnological relevant host (Figure 7). Overexpression of magnetosome genes substantially increased overall magnetosome yields (Figure 7A). For instance, combined duplication of the major operons *mms6_{op}*, *mamGFDC_{op}*, *mamAB_{op}* and *mamXY_{op}* comprising nearly all about 30 known magnetosome genes caused a 2.5-fold increased iron accumulation and a 2.2-fold increased number of crystals per cell. Such merodiploidic overproducers are very promising for the biotechnological mass production of magnetosomes.²⁹ In addition, *Kolinko et al. (2014)* succeeded for the first time in transplantation of bacterial magnetosome gene clusters and even the entire pathway of magnetosome biosynthesis to a foreign organism (Figure 7B).⁷⁴ Transfer of about 30 genes from *M. gryphiswaldense* to the nonmagnetic, photosynthetic model organism *Rhodospirillum rubrum* induced biosynthesis of well-ordered magnetosome chains. Importantly, mutant phenotypes known from the donor *M. gryphiswaldense* could also be replicated, thus rendering the synthetic *R. “magneticum”* a promising alternative for generation of genetically engineered bioconjugated magnetosomes. This demonstrates that *mam* genes or whole operons can be transferred to organisms that are easier to cultivate and allow high yield production of (functionalized) magnetosomes.

7. Conclusion and outlook

In a systematic stepwise bottom-up approach, we identified magnetosome proteins with

biomineralizing activity and delineated a model for magnetosome biosynthesis, thus enabling the generation of core-engineered particles with defined physico-chemical properties by synthetic biology approaches.^{15,16} As many biotechnological and biomedical applications would benefit from multimodal particles with genetically encoded and tunable characteristics, versatile expression systems were developed that allowed the generation of tailored, multifunctional magnetosomes (Figure 8). The feasibility and power of this bionic “Swiss army knife” was demonstrated by the production of a set of different model particles. Clearly, this high degree of control can only be achieved by molecular-genetic approaches (i.e. by harnessing magnetosome membrane proteins as anchors for versatile protein-based/-derived functions) and is inaccessible by inorganic synthesis.

These strategies therefore provide highly promising routes for the stable expression and immobilization of functional moieties, as the display (and reusability) of, for instance, catalytically active enzymes are still common challenges.⁷⁵ The properties of magnetic biosensors and protein arrays for drug screening are based on the efficient immobilization of (enzyme) proteins, and a high degree of control over the immobilization process is required,^{76,77} which makes genetically engineered magnetosomes to an attractive platform for the high-level display of foreign proteins. Magnetosome display of molecular connectors might be furthermore used for the generation of (multi)functionalized hybrid composites that could be used as novel biomaterials.⁴⁰ In addition, inorganic and organic encapsulation strategies would not only significantly improve stability of the expressed moieties, but also mask immunogenic compounds and improve biocompatibility of the particles for future *in vivo*

applications.^{42,68} Overall, this illustrates the versatile features of engineered bacterial magnetosomes, providing routes toward the generation of fully genetically encoded functionalized hybrid composites that might be useful as novel biomaterials with enhanced properties in biotechnological/biomedical and research applications.

Acknowledgements

We are grateful to A. Lohße for providing TEM micrographs of *M. gryphiswaldense* cells and statistics on magnetosome particle numbers, and D. Maier for providing TEM micrographs of silica-coated magnetosomes. M. Toro-Nahuelpan is acknowledged for performing 3D rendering of tomographed spider silk-expressing cells. We thank all our collaborators, in particular J. Bill, D. Rothenstein, C. Wege (University of Stuttgart), D. Zahn (University of Erlangen), D. Faivre (Max-Planck-Institut für Kolloid- und Grenzflächenforschung, Potsdam-Golm), N. Kröger (University of Dresden), and T. Scheibel (University of Bayreuth). This project was supported by grants from the Deutsche Forschungsgemeinschaft (Schu1080/15-1, 15-2 and 15-3) and the European Research Council (ERC AdG Syntomagx) to Dirk Schüler.

References

1. Prozorov T, Bazylinski DA, Mallapragada SK and Prozorov R (2013) Novel magnetic nanomaterials inspired by magnetotactic bacteria. *Mater. Sci. Eng. R Rep.* **74(5)**: 1-40.
2. Komeili A (2012) Molecular mechanisms of compartmentalization and biomineralization in magnetotactic bacteria. *FEMS Microbiol. Rev.* **36(1)**: 232-55.
3. Uebe R and Schüler D (2016) Magnetosome biogenesis in magnetotactic bacteria. *Nat. Rev. Microbiol.* **14**: 621-37.
4. Jogler C and Schüler D (2009) Genomics, genetics, and cell biology of magnetosome formation. *Annu. Rev. Microbiol.* **63**: 501-21.
5. Staniland SS and Rawlings AE (2016) Crystallizing the function of the magnetosome membrane mineralization protein Mms6. *Biochem. Soc. Trans.* **44(3)**: 883-90.
6. Faivre D and Schüler D (2008) Magnetotactic bacteria and magnetosomes. *Chemical. Rev.* **108(11)**: 4875-98.
7. Taukulis R, Widdrat M, Kumari M, Heinke D, Rumpler M, Tompa É, Uebe R, Kraupner A, Cebers A, Schüler D, Pósfai M, Hirt A and Faivre D (2015) Magnetic iron oxide nanoparticles as MRI contrast agents - a comprehensive physical and theoretical study. *MHD* **51(4)**: 721-47.
8. Kraupner A, Eberbeck D, Heinke D, Uebe R, Schüler D and Briel A (2017) Bacterial magnetosomes - nature's powerful contribution to MPI tracer research. *Nanoscale*, **9(18)**: 5788-93.

9. Heinke D, Kraupner A, Eberbeck D, Schmidt D, Radon P, Uebe R, Schüler D and Briel A (2017) MPS and MRI efficacy of magnetosomes from wild-type and mutant bacterial strains. *IJMPI* **3(2)**: 1706004.
10. Lisy MR, Hartung A, Lang C, Schüler D, Richter W, Reichenbach JR, Kaiser WA and Hilger I (2007) Fluorescent bacterial magnetic nanoparticles as bimodal contrast agents. *Invest. Radiol.* **42(4)**: 235-41.
11. Schwarz S, Fernandes F, Sanroman L, Hodenius M, Lang C, Himmelreich U, Fama G, Schmitz-Rode T, Schüler D, Hoehn M, Zenke M and Hieronymus T (2009) Synthetic and biogenic magnetite nanoparticles for tracking of stem cells and dendritic cells. *J. Magn. Mater.* **321(10)**: 1533-8.
12. Hergt R, Hiergeist R, Zeisberger M, Schüler D, Heyen U, Hilger I and Kaiser WA (2005) Magnetic properties of bacterial magnetosomes as potential diagnostic and therapeutic tools. *J. Magn. Mater.* **293**: 80-6.
13. Alphandéry E, Guyot F and Chebbi I (2012) Preparation of chains of magnetosomes, isolated from *Magnetospirillum magneticum* strain AMB-1 magnetotactic bacteria, yielding efficient treatment of tumors using magnetic hyperthermia. *Int. J. Pharm.* **434(1-2)**: 444-52.
14. Schüler D (2008) Genetics and cell biology of magnetosome formation in magnetotactic bacteria. *FEMS Microbiol. Rev.* **32(4)**: 654-72.
15. Lohße A, Ullrich S, Katzmann E, Borg S, Wanner G, Richter M, Voigt B, Schweder T and Schüler D (2011) Functional analysis of the magnetosome island in *Magnetospirillum*

- gryphiswaldense: the mamAB operon is sufficient for magnetite biomineralization. *PLoS One* **6(10)**: e25561.
16. Lohße A, Borg S, Raschdorf O, Kolinko I, Tompa E, Pósfai M, Faivre D, Baumgartner J and Schüler D (2014) Genetic dissection of the mamAB and mms6 operons reveals a gene set essential for magnetosome biogenesis in *Magnetospirillum gryphiswaldense*. *J. Bacteriol.* **196(14)**: 2658-69.
17. Raschdorf O, Forstner Y, Kolinko I, Uebe R, Plitzko JM and Schüler D (2016) Genetic and ultrastructural analysis reveals the key players and initial steps of bacterial magnetosome membrane biogenesis. *PLoS genet.* **12(6)**: e1006101.
18. Uebe R, Junge K, Henn V, Poxleitner G, Katzmann E, Plitzko JM, Zarivach R, Kasama T, Wanner G, Pósfai M, Bottger L, Matzanke B and Schüler D (2011) The cation diffusion facilitator proteins MamB and MamM of *Magnetospirillum gryphiswaldense* have distinct and complex functions, and are involved in magnetite biomineralization and magnetosome membrane assembly. *Mol. Microbiol.* **82(4)**: 818-35.
19. Raschdorf O, Müller FD, Pósfai M, Plitzko JM and Schüler D (2013) The magnetosome proteins MamX, MamZ and MamH are involved in redox control of magnetite biomineralization in *Magnetospirillum gryphiswaldense*. *Mol. Microbiol.* **89(5)**: 872-86.
20. Quinlan A, Murat D, Vali H and Komeili A (2011) The HtrA/DegP family protease MamE is a bifunctional protein with roles in magnetosome protein localization and magnetite biomineralization. *Mol. Microbiol.* **80(4)**: 1075-87.

21. Siponen MI, Adryanczyk G, Ginet N, Arnoux P and Pignol D (2012) Magnetochrome: a c-type cytochrome domain specific to magnetotactic bacteria. *Biochem. Soc. Trans.* **40(6)**: 1319-23.
22. Oestreicher Z, Valverde-Tercedor C, Chen L, Jimenez-Lopez C, Bazylinski DA, Casillas-Ituarte NN, Lower SK and Lower BH (2012) Magnetosomes and magnetite crystals produced by magnetotactic bacteria as resolved by atomic force microscopy and transmission electron microscopy. *Micron* **43(12)**: 1331-5.
23. Tanaka M, Mazuyama E, Arakaki A and Matsunaga T (2011) MMS6 protein regulates crystal morphology during nano-sized magnetite biomineralization in vivo. *J. Biol. Chem.* **286(8)**: 6386-92.
24. Scheffel A, Gärdes A, Grünberg K, Wanner G and Schüler D (2008) The major magnetosome proteins MamGFDC are not essential for magnetite biomineralization in *Magnetospirillum gryphiswaldense*, but regulate the size of magnetosome crystals. *J. Bacteriol.* **190(1)**: 377-86.
25. Scheffel A and Schüler D (2007) The acidic repetitive domain of the *Magnetospirillum gryphiswaldense* MamJ protein displays hypervariability but is not required for magnetosome chain assembly. *J. Bacteriol.* **189(17)**: 6437-46.
26. Toro-Nahuelpan M, Müller FD, Klumpp S, Plitzko JM, Bramkamp M and Schüler D (2016) Segregation of prokaryotic magnetosomes organelles is driven by treadmilling of a dynamic actin-like MamK filament. *BMC biology* **14(1)**: 88.

27. Kumari M, Widdrat M, Tompa É, Uebe R, Schüler D, Pósfai M, Faivre D and Hirt AM (2014) Distinguishing magnetic particle size of iron oxide nanoparticles with first-order reversal curves. *J. Appl. Phys.* **116(12)**: 124304.
28. Bennet M, Bertinetti L, Neely RK, Schertel A, Körnig A, Flors C, Müller FD, Schüler D, Klumpp S and Faivre D (2015) Biologically controlled synthesis and assembly of magnetite nanoparticles. *Faraday discuss.* **181**: 71-83.
29. Lohsse A, Kolinko I, Raschdorf O, Uebe R, Borg S, Brachmann A, Plitzko JM, Müller R, Zhang Y and Schüler D (2016) Overproduction of magnetosomes by genomic amplification of biosynthesis-related gene clusters in a magnetotactic bacterium. *Appl. Environ. Microbiol.* **82(10)**: 3032-41.
30. Kolinko I, Jogler C, Katzmann E and Schüler D (2011) Frequent mutations within the genomic magnetosome island of *Magnetospirillum gryphiswaldense* are mediated by RecA. *J. Bacteriol.* **193(19)**: 5328-34.
31. Sapsford KE, Algar WR, Berti L, Gemmill KB, Casey BJ, Oh E, Stewart MH and Medintz IL (2013) Functionalizing nanoparticles with biological molecules: developing chemistries that facilitate nanotechnology. *Chem. Rev.* **113(3)**: 1904-2074.
32. Grünberg K, Müller EC, Otto A, Reszka R, Linder D, Kube M, Reinhardt R and Schüler D (2004) Biochemical and proteomic analysis of the magnetosome membrane in *Magnetospirillum gryphiswaldense*. *Appl. Environ. Microbiol.* **70(2)**: 1040-50.

33. Lang C and Schüler D (2008) Expression of green fluorescent protein fused to magnetosome proteins in microaerophilic magnetotactic bacteria. *Appl. Environ. Microbiol.* **74(5)**: 4944-53.
34. Borg S, Hofmann J, Pollithy A, Lang C and Schüler D (2014) New vectors for chromosomal integration enable high-level constitutive or inducible magnetosome expression of fusion proteins in *Magnetospirillum gryphiswaldense*. *Appl. Environ. Microbiol.* **80(8)**: 2609-16.
35. Nudelman H and Zarivach R (2014) Structure prediction of magnetosome-associated proteins. *Front. Microbiol.* **5**: 9.
36. Bertram R and Hillen W (2008) The application of Tet repressor in prokaryotic gene regulation and expression. *Microb. Biotechnol.* **1**: 2-16.
37. Raschdorf O, Bonn F, Zeytuni N, Zarivach R, Becher D and Schüler D (2018) A quantitative assessment of the membrane-integral sub-proteome of a bacterial magnetic organelle. *J. Proteom.* **172**: 89-99.
38. Mickoleit F and Schüler D (2016) Poster @Annual Conference 2016 of the Association for General and Applied Microbiology (VAAM), Jena, Germany. Functionalization of magnetosomes from *Magnetospirillum gryphiswaldense* by *in vivo* surface display of functional groups and reporter enzymes: BTP34.
39. Mickoleit F and Schüler D (2018) Generation of multifunctional magnetic nanoparticles with amplified catalytic activities by genetic expression of enzyme arrays on bacterial magnetosomes. *Adv. Biosyst.* **2(1)**: 1700109.

40. Mickoleit F, Altintoprak K, Wenz NL, Wege C and Schüler D Controlled assembly of functionalized magnetosomes and tobacco mosaic virus particles generates magnetic biocomposites. *Manuscript in preparation*.
41. Ohuchi S and Schüler D (2009) In vivo display of a multisubunit enzyme complex on biogenic magnetic nanoparticles. *Appl. Environ. Microbiol.* **75(24)**: 7734-8.
42. Mickoleit F, Borkner CB, Toro-Nahuelpan M, Herold HM, Maier DS, Plitzko J, Scheibel T and Schüler D (2018) In vivo coating of bacterial magnetic nanoparticles by magnetosome expression of spider silk-inspired peptides. *Biomacromolecules*, doi: 10.1021/acs.biomac.7b01749.
43. Baer MF, Wesolowski D and Altman S (1989) Characterization in vitro of the defect in a temperature-sensitive mutant of the protein subunit of RNase P from *Escherichia coli*. *J. Bacteriol.* **171(12)**: 6862-6.
44. Li Y, Katzmann E, Borg S and Schüler D (2012) The periplasmic nitrate reductase Nap is required for anaerobic growth and involved in redox control of magnetite biomineralization in *Magnetospirillum gryphiswaldense*. *J. Bacteriol.* **194(18)**: 4847-56.
45. Li Y, Sabaty M, Borg S, Silva KT, Pignol D and Schüler D (2014) The oxygen sensor MgFnr controls magnetite biomineralization by regulation of denitrification in *Magnetospirillum gryphiswaldense*. *BMC Microbiol.* **14**: 153.
46. Pollithy A, Romer T, Lang C, Müller FD, Helma J, Leonhardt H, Rothbauer U and Schüler D (2011) Magnetosome expression of functional camelid antibody fragments (nanobodies) in *Magnetospirillum gryphiswaldense*. *Appl. Environ. Microbiol.* **77(17)**: 6165-71.

47. Borg S, Popp F, Hofmann J, Leonhardt H, Rothbauer U and Schüler D (2015) An intracellular nanotrap redirects proteins and organelles in live bacteria. *MBio*. **6(1)** pii: e02117-14.
48. Jehle F, Valverde-Tercedor C, Reichel V, Carillo MA, Bennet M, Günther E, Wirth R, Mickoleit F, Zarivach R, Schüler D, Blank KG and Faivre D (2017) Genetically engineered organization: protein template, biological recognition sites, and nanoparticles. *Adv. Mater. Interfaces* **4(1)**: 1600285.
49. Ceyhan B, Alhorn P, Lang C, Schüler D and Niemeyer CM (2006) Semisynthetic biogenic magnetosome nanoparticles for the detection of proteins and nucleic acids. *SMALL* **2**: 1251-5.
50. Lang C, Schüler D and Faivre D (2007) Synthesis of magnetite nanoparticles for bio- and nanotechnology: genetic engineering and biomimetics of bacterial magnetosomes. *Macromol. Biosci.* **7(2)**: 144-51.
51. Tanaka T, Maruyama K, Yoda K, Nemoto E, Udagawa Y, Nakayama H, Takeyama H and Matsunaga T (2003) Development and evaluation of an automated workstation for single nucleotide polymorphism discrimination using bacterial magnetic particles. *Biosens. Bioelectron.* **19(4)**: 325-30.
52. Shukla S and Steinmetz NF (2015) Virus-based nanomaterials as positron emission tomography and magnetic resonance contrast agents: from technology development to translational medicine. *Wiley Interdiscip. Rev. Nanomed. Nanobiotechnol.* **7(5)**: 708-21.

53. Koch C, Eber FJ, Azucena C, Förste A, Walheim S, Schimmel T, Bittner AM, Jeske H, Gliemann H, Eiben S, Geiger FC and Wege C (2016) Novel roles for well-known players: from tobacco mosaic virus pests to enzymatically active assemblies. *Beilstein J. Nanotechnol.* **7**: 613.
54. Smith ML, Lindbo JA, Dillard-Telm S, Brosio PM, Lasnik AB, McCormick AA, Nguyen LV and Palmer KE (2006) Modified tobacco mosaic virus particles as scaffolds for display of protein antigens for vaccine applications. *Virology* **348(2)**: 475-88.
55. Wu Z, Mueller A, Degenhard S, Ruff SE, Geiger F, Bittner AM, Wege C and Krill III CE (2010) Enhancing the magnetoviscosity of ferrofluids by the addition of biological nanotubes. *ACS nano* **4(8)**: 4531-8.
56. Culver JN, Brown AD, Zang F, Gnerlich M, Gerasopoulos K and Ghodssi R (2015) Plant virus directed fabrication of nanoscale materials and devices. *Virology* **479**: 200-12.
57. Vollrath F (2000) Strength and structure of spiders' silks. *Rev. Mol. Biotechnol.* **74(2)**: 67-83.
58. Bini E, Knight DP and Kaplan DL (2004) Mapping domain structures in silks from insects and spiders related to protein assembly. *J. Mol. Biol.* **335(1)**: 27-40.
59. Leal-Egaña A and Scheibel T (2010) Silk-based materials for biomedical applications. *Biotechnol. Appl. Biochem.* **55(3)**: 155-67.
60. Huemmerich D, Helsen CW, Quedzuweit S, Oschmann J, Rudolph R and Scheibel T (2004) Primary structure elements of spider dragline silks and their contribution to protein solubility. *Biochemistry* **43(42)**: 13604-12.

61. Rammensee S, Slotta U, Scheibel T and Bausch AR (2008) Assembly mechanism of recombinant spider silk proteins. *Proc. Natl. Acad. Sci. U.S.A.* **105(18)**: 6590-5.
62. Sabourin M, Tuzon C, Fisher T and Zakian VA (2007) Flexible protein linker improves the function of epitope-tagged proteins in *Saccharomyces cerevisiae*. *Yeast* **24(1)**: 39-45.
63. Humenik M, Magdeburg M and Scheibel T (2014) Influence of repeat numbers on self-assembly rates of repetitive recombinant spider silk proteins. *J. Struct. Biol.* **186(3)**: 431-7.
64. Zbilut JP, Scheibel T, Huemmerich D, Webber CL Jr, Colafranceschi M and Giuliani A (2006) Statistical approaches for investigating silk properties. *Appl. Phys. A* **82(2)**: 243-51.
65. Zbilut JP, Scheibel T, Huemmerich D, Webber CL Jr, Colafranceschi M and Giuliani A (2005) Spatial stochastic resonance in protein hydrophobicity. *Phys. Lett. A* **346(1-3)**: 33-41.
66. Spiess K, Lammel A and Scheibel T (2010) Recombinant spider silk proteins for applications in biomaterials. *Biosci.* **10(9)**: 998-1007.
67. Mayes EL, Vollrath F and Mann S (1998) Fabrication of magnetic spider silk and other silk-fiber composites using inorganic nanoparticles. *Adv. Mater.* **10(10)**: 801-5.
68. Borg S, Rothenstein D, Bill J and Schüler D (2015) Generation of multishell magnetic hybrid nanoparticles by encapsulation of genetically engineered and fluorescent bacterial magnetosomes with ZnO and SiO₂. *SMALL* **11(33)**: 4209-17.
69. Rothenstein D, Claasen B, Omiecienski B, Lammel P and Bill J (2012) Isolation of ZnO-binding 12-mer peptides and determination of their binding epitopes by NMR spectroscopy. *J. Am. Chem. Soc.* **134(30)**: 12547-56.

70. Gao PX and Wang ZL (2005) Nanoarchitectures of semiconducting and piezoelectric zinc oxide. *J. Appl. Phys.* **97**: 044304.
71. Jones N, Ray B, Ranjit KT and Manna AC (2008) Antibacterial activity of ZnO nanoparticle suspensions on a broad spectrum of microorganisms. *FEMS Microbiol. Lett.* **279(1)**: 71-6.
72. Zhang Y, Zhang X, Jiang W, Li Y and Li J (2011) Semicontinuous culture of *Magnetospirillum gryphiswaldense* MSR-1 cells in an autofermentor by nutrient-balanced and isosmotic feeding strategies. *Appl. Environ. Microbiol.* **77(17)**: 5851-6.
73. Heyen U and Schüler D (2003) Growth and magnetosome formation by microaerophilic *Magnetospirillum* strains in an oxygen-controlled fermentor. *Appl. Microbiol. Biotechnol.* **61(5-6)**: 536-44.
74. Kolinko I, Lohße A, Borg S, Raschdorf O, Jogler C, Tu Q, Pósfai M, Tompa E, Plitzko JM, Brachmann A, Wanner G, Müller R, Zhang Y and Schüler D (2014) Biosynthesis of magnetic nanostructures in a foreign organism by transfer of bacterial magnetosome gene clusters. *Nat. Nanotechnol.* **9(3)**: 193-7.
75. Narancic T, Davis R, Nikodinovic-Runic J and O'Connor KE (2015) Recent developments in biocatalysis beyond the laboratory. *Biotechnol. Lett.* **37(5)**: 943-54.
76. Liang JF, Li YT and Yang VC (2000) Biomedical application of immobilized enzymes. *J. Pharm. Sci.* **89(8)**: 979-90.
77. Meldal M and Schoffelen S (2016) Recent advances in covalent, site-specific protein immobilization. *F1000Research* **5**: 2303.

Figure 1. Formation and arrangement of magnetosomes in *M. gryphiswaldense*. (A) Transmission electron micrograph of a wild type cell of *M. gryphiswaldense*. Electron dense particles are magnetite crystals (on average 35 nm in diameter), which are chain-like arranged within the cell. (B) Suspensions of isolated magnetosomes (obtained from microoxic cultivated wild type cells of *M. gryphiswaldense*) were free of contamination, uniform, and contained well dispersed particles. (C) TEM micrograph and (D) schematic illustration of magnetosome nanoparticles, consisting of a monocrystalline magnetite core enveloped by the magnetosome membrane, which harbours a set of specialized proteins.

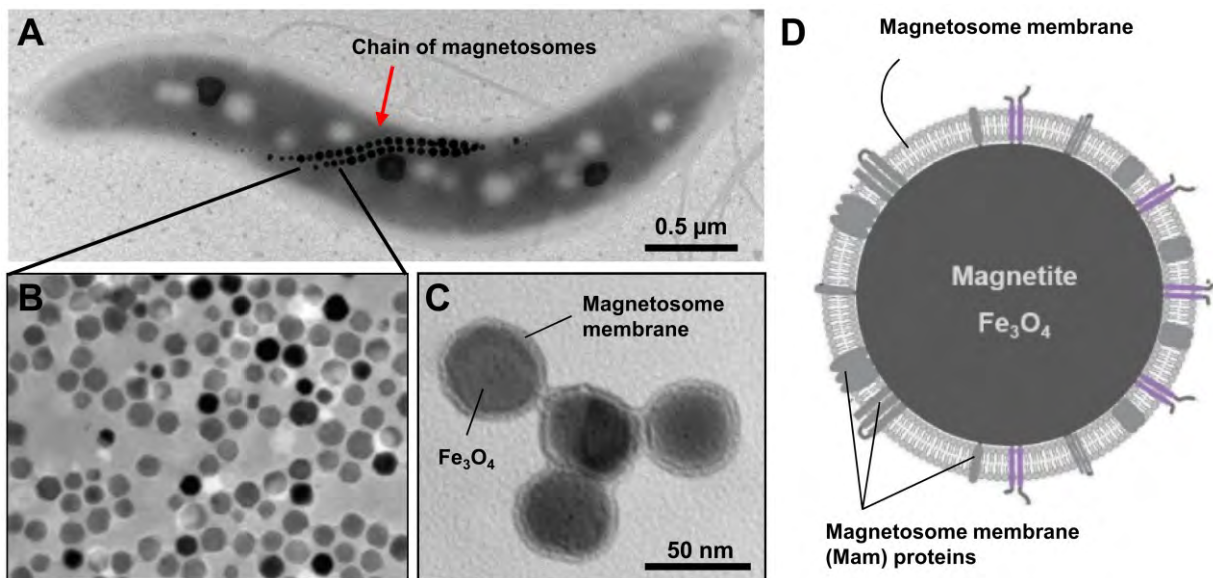


Figure 2. Magnetosome biosynthesis in *M. gryphiswaldense*. (A) Molecular organization of the genomic magnetosome island (MAI), which contains genes with specific functions in magnetosome biogenesis organized into five operons (*mms6*_{OP}, *mamGFDC*_{OP}, *mamAB*_{OP}, *mamXY*_{OP}, and *feoAB1*_{OP}). (B) Current hypothetical model of iron uptake, magnetite crystal nucleation and crystal maturation in *M. gryphiswaldense*.^{3,16} The subsequent assembly of magnetosome chains is controlled by MamK-MamJ interactions (not shown).^{25,26} For details refer to the text

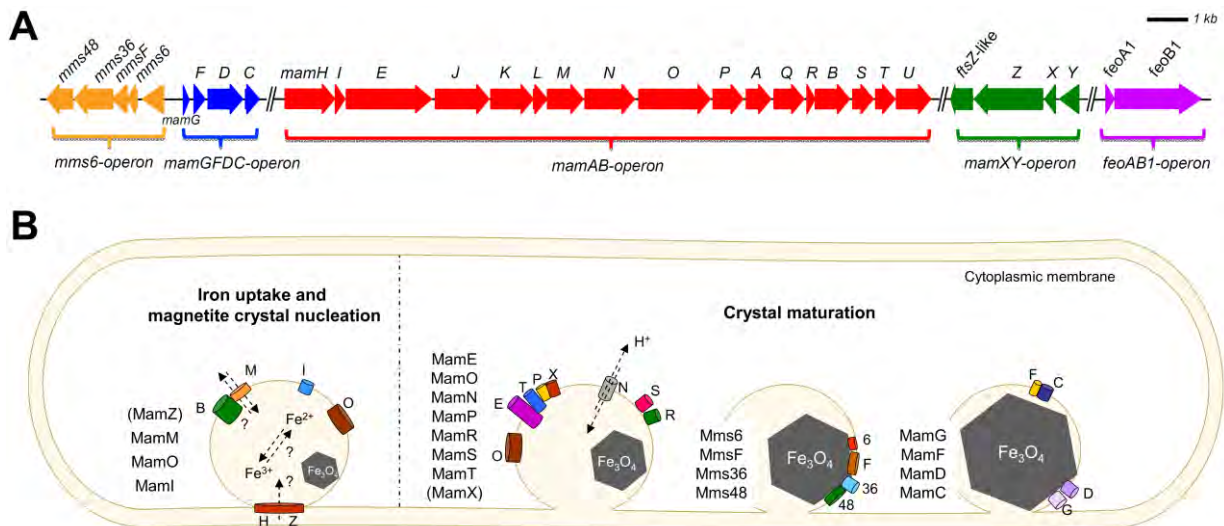


Figure 3. TEM micrographs of magnetosomes isolated from selected *M. gryphiswaldense* strains and size/volume dependent magnetic response (coercivity). The magnetic response depends on the magnetosome size and volume. Due to the particle diameter, different coercivity conditions can be distinguished. Particles with diameters ranging from 5-30 nm exhibit superparamagnetic (SP) behavior, while magnetosomes between 30 and 60-100 nm are stable single domain (SSD). Large single domain particles (LSD) represent an optimum, close to maximal coercivity, and particles larger than 100 nm being multidomain (MD, more than one domain).^{7,27,28} Strain $\Delta F3D$ exhibited the dominance of magnetic particles that are SP whereas WT and $\Delta mms48$ contain a broader mixture of SP and SSD particles (TEM images of strains $\Delta F3D$, WT and $\Delta mms48$ modified from Ref. 7, coercivity diagram adapted from Ref. 28. For strain $2x mms6$ (an overproducing strain which contains an extra copy of the *mms6* operon), a high portion of SSD particles was obtained

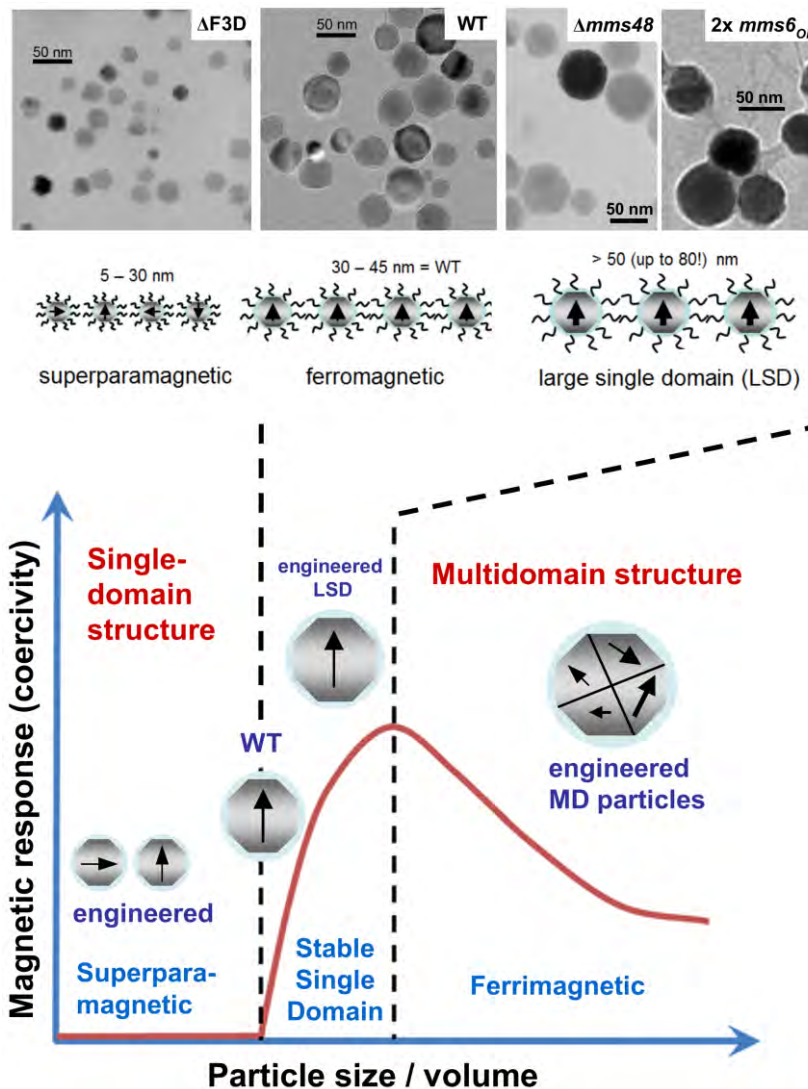


Figure 4. (Multi-)Functionalization of bacterial magnetosomes from *M. gryphiswaldense* (selection) by synthetic biology approaches. Using an optimized expression cassette,³⁴ a set of surface-functionalized magnetic particles was created. The highly abundant magnetosome membrane protein MamC was used as membrane anchor for the display of foreign proteins and peptides, expressed as large hybrid proteins. (1) Magnetosome expression of *mamC*-(*gusA*)_n-*megfp* fusions resulted in particles that display arrays of one to five copies of the glucuronidase GusA and mEGFP (codon-optimized eGFP) as fluorophore.³⁹ MamC, GusA monomers, and mEGFP were fused via Gly₁₀ linkers (composed of ten glycine residues). Catalytic GusA activities were step-wise increased with the number of GusA monomers, and expressed arrays covered up to 90% of the particle surface (TEM micrographs adapted from Ref. 39). (2) Display of GBP nanobodies or streptavidin (SAV) produced as hybrid-proteins fused to a single MamC membrane anchor. GBP or SAV magnetosomes allowed specific coupling with GFP- or biotin-functionalized tobacco mosaic virus (TMV) particles, thereby generating mesoscopic, strand-like TMV-magnetosome composites, or even ‘drumstick’-like structures.⁴⁰ (3) Display of RNase P on magnetosomes. The protein subunit (C5) of *E. coli* RNase P was fused to the C-terminus of MamC via 13 residues of a flexible Gly-Ser linker. Isolated C5 particles showed apparent RNase P activity and could associate with the endogenous RNase P RNA subunit.⁴¹ (4) Magnetosome expression of spider silk-inspired sequences resulted in the generation of an organic/proteinaceous capsule and significantly improved colloidal stability of the particles.⁴² For details refer to the text. Size of particles and proteins not to scale

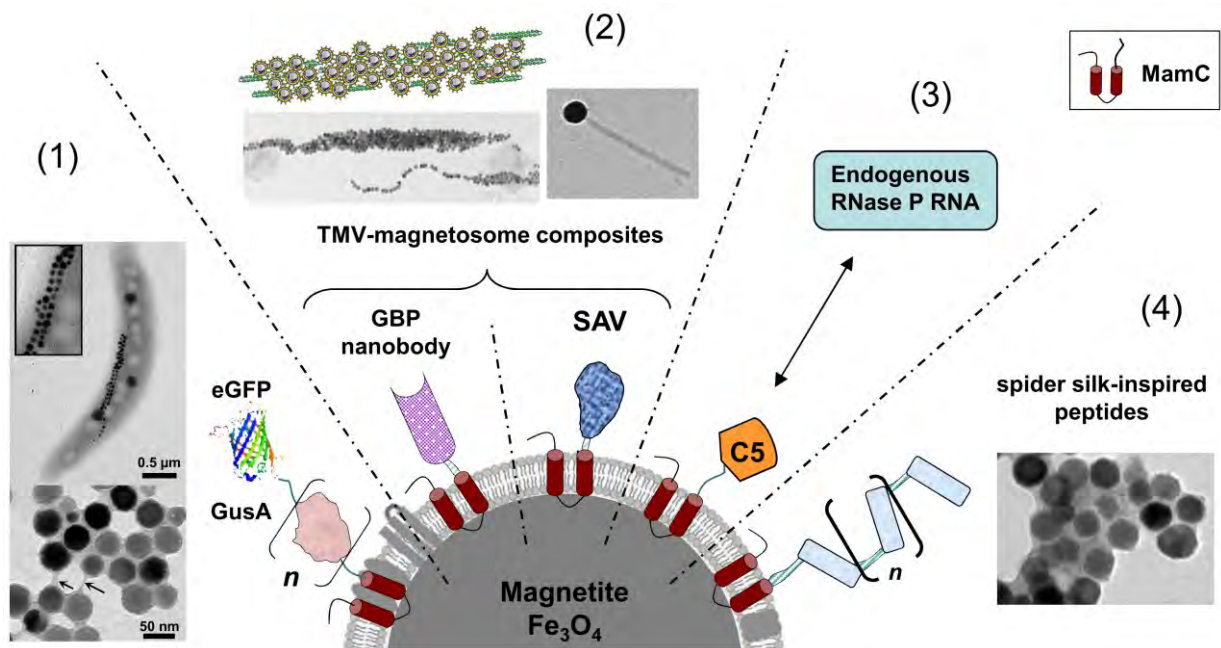


Figure 5. Display of spider silk-inspired peptides on magnetosomes of *M. gryphiswaldense*.⁴² Genetic fusion of different silk sequence-like variants to the abundant magnetosome membrane protein MamC enhanced magnetite biomineralization and caused the formation of a proteinaceous capsule. Depending on the hybrid protein displayed on the particle surface, cells partially seemed to be caught in cytokinesis and tended to form minicell-like structures at the division sites, before becoming eventually separated. Cryo-electron tomography was used to investigate the subcellular ultrastructure in a near-native state. (Cryo-electron tomogram and CET 3D rendering by M. Toro-Nahuelpan)

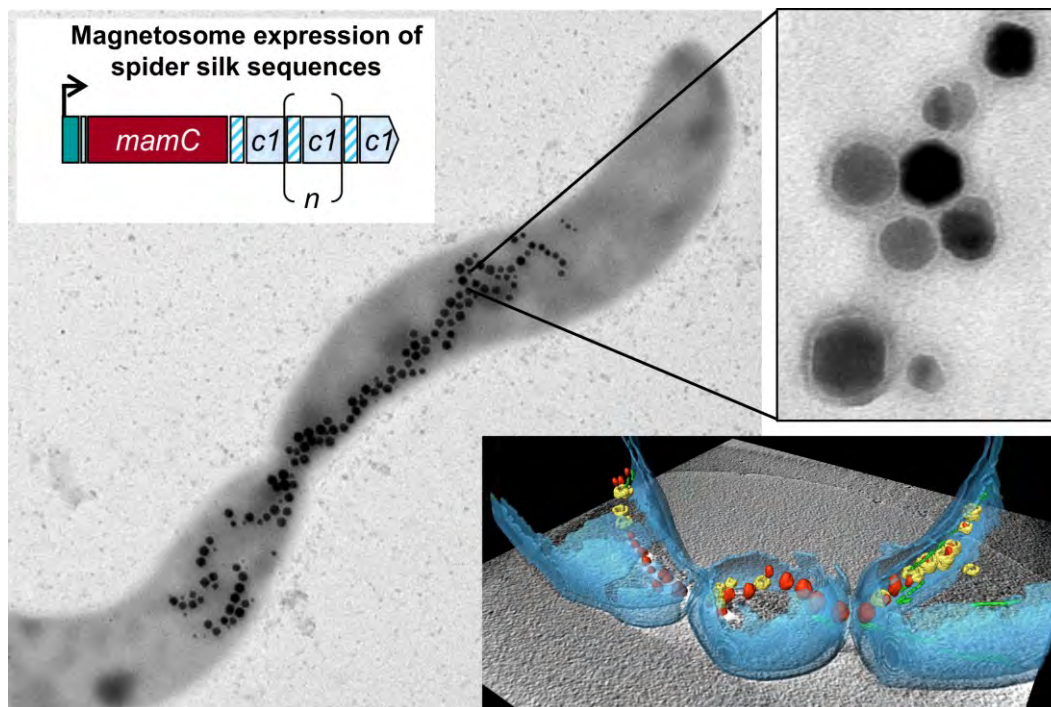


Figure 6. Silica-encapsulation of isolated magnetosomes from *M. gryphiswaldense*. (A) Transmission electron micrographs of purified WT magnetosomes. Particles were surrounded by an organic layer of about 5 nm, representing the magnetosome membrane. (B) Experimental setup for silica-encapsulation.⁶⁸ Tetraethyl orthosilicate (TEOS) was precipitated in alkaline solution using isolated magnetosomes as precursor. Incubation for 18-24 h resulted in the formation of silica-shelled particles. (C) TEM micrographs of silica-encapsulated magnetosomes. In the absence of an external magnetic field layer thicknesses ranging from 10-60 nm were observed. (TEM micrographs by D. Maier)

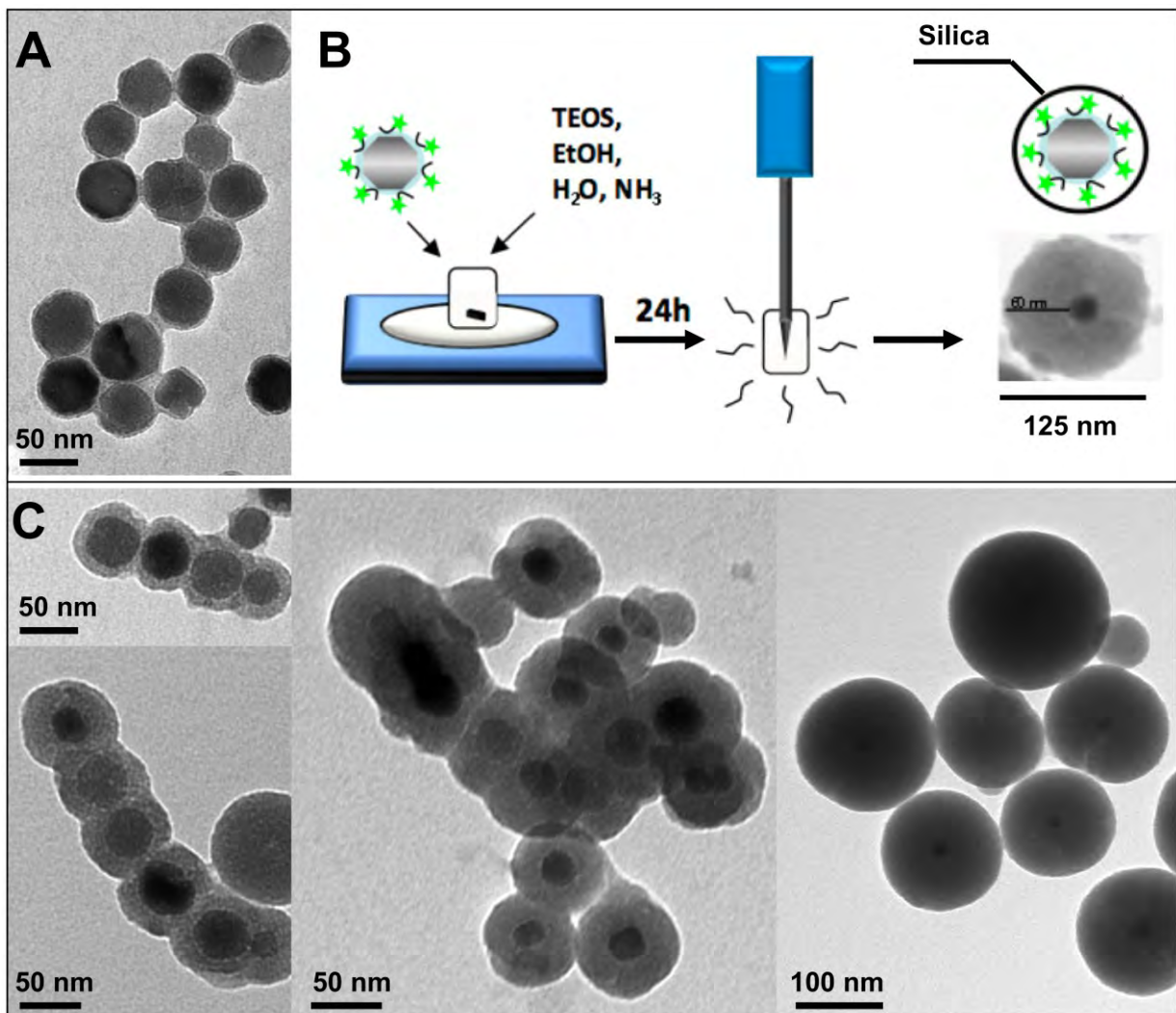


Figure 7. Generation of magnetosome overproducing strains and magnetosome production in a foreign host by synthetic biology approaches. (A) Overexpression of magnetosome genes or whole operons by genomic multiplication substantially increased crystal sizes (up to 15%) and particle yields (up to 120%). Overproducing cells contained 75 electron-dense particles on average (increase in number by 120%). About 30% of cells had more than 100 magnetosomes (maximum number: 169) and most cells contained multiple (two to four) magnetosome chains.²⁹ (B) Transplantation of the entire pathway of magnetosome biosynthesis from *M. gryphiswaldense* to the nonmagnetic, photosynthetic model organism *Rhodospirillum rubrum* induced biosynthesis of well-ordered magnetosome chains (up to 30 particles per cell).⁷⁴ Unlike the untransformed *R. rubrum* wild type, cells of *R. “magneticum”* accumulated as a visible red spot near the pole of a permanent magnet at the edge of a culture flask. In suspensions of isolated magnetosomes, particles with intact membranes were visible

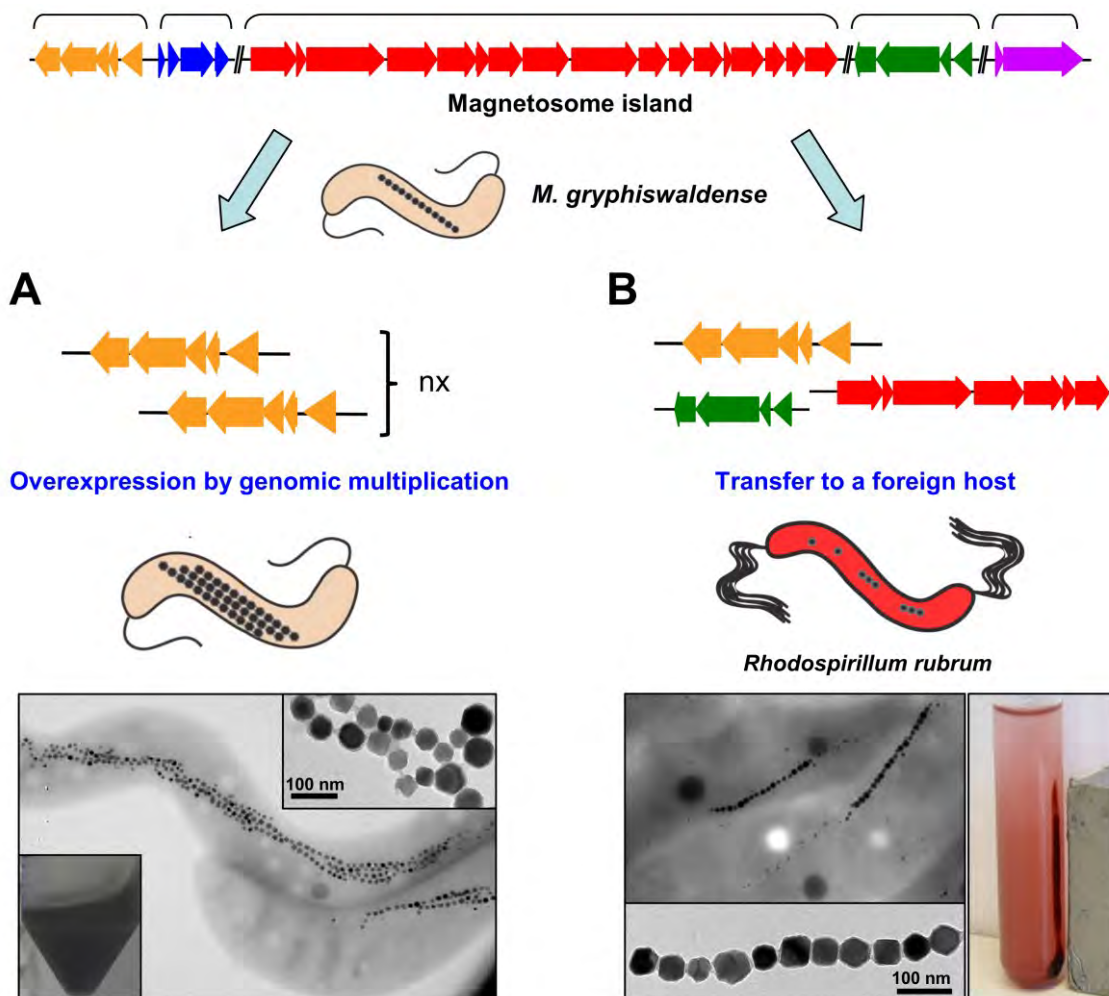


Figure 8. Generation of multifunctional core-engineered, bacterial nanoparticles by synthetic biology, and their application potential. Using optimized expression cassettes,³⁴ highly abundant magnetosome membrane proteins are utilized as membrane anchors for the display of an unprecedented set of (improved) functionalities comprising fluorophores (like GFP, RFP and variants) that allow tracking and detection,^{33,34,39} (reporter-)enzymes (e.g. the glucuronidase *GusA*, or glucose oxidase *GOx*) for the use as biosensors,³⁹ chemically and biologically stable coupling groups/tags like streptavidin (SAV) for the generation of new kinds of biocomposites,⁴⁰ anti-/nanobodies for specific ligand/antigen targeting,^{46,47} and metal precipitating peptides. Inorganic encapsulation strategies (e.g. silica-coating) were shown to improve enzyme stability and are supposed to enhance biocompatibility.⁶⁸

